

UCRL-JRNL-221120



LAWRENCE
LIVERMORE
NATIONAL
LABORATORY

3w Transmitted Beam Diagnostic at the Omega Laser Facility

D. H. Froula, V. Rekow, C. Sorce, K. Piston, R. Knight, S. Alvarez, R. Griffith, D. Hargrove, J. S. Ross, S. Dixit, B. Pollock, L. Divol, S. H. Glenzer, W. Armstrong, K. Thorp, G. Pien

May 5, 2006

Review of Scientific Instruments

Disclaimer

This document was prepared as an account of work sponsored by an agency of the United States Government. Neither the United States Government nor the University of California nor any of their employees, makes any warranty, express or implied, or assumes any legal liability or responsibility for the accuracy, completeness, or usefulness of any information, apparatus, product, or process disclosed, or represents that its use would not infringe privately owned rights. Reference herein to any specific commercial product, process, or service by trade name, trademark, manufacturer, or otherwise, does not necessarily constitute or imply its endorsement, recommendation, or favoring by the United States Government or the University of California. The views and opinions of authors expressed herein do not necessarily state or reflect those of the United States Government or the University of California, and shall not be used for advertising or product endorsement purposes.

3ω Transmitted Beam Diagnostic at the Omega Laser Facility

D. H. Froula, V. Rekow, C. Sorce, K. Piston, R. Knight, S. Alvarez, R. Griffith,
D. Hargrove, J. S. Ross, S. Dixit, B. Pollock, L. Divol, and S. H. Glenzer

Lawrence Livermore National Laboratory, University of California, P.O. Box 808, Livermore, California 94551

W. Armstrong, R. Bahr, K. Thorp, and G. Pien

Laboratory for Laser Energetics, 250 E. River Rd., Rochester, New York 14623

A 3ω transmitted beam diagnostic has been commissioned on the Omega Laser at the Laboratory for Laser Energetics, University of Rochester [Soures *et.al.*, Laser Part. Beams **11** (1993)]. Transmitted light from one beam is collected by a large focusing mirror and directed onto a diagnostic platform. The near field of the transmitted light is imaged; the system collects information from twice the original f-cone of the beam. Two gated optical cameras capture the near field image of the transmitted light. Thirteen spatial positions around the measurement region are temporally resolved using fast photodiodes to allow a measure of the beam spray evolution. The Forward stimulated Raman scattering and forward simulated Brillouin scattering are spectrally and temporally resolved at 5 independent locations within twice the original f-cone. The total transmitted energy is measured in two spectral bands ($\delta\lambda < 400$ nm and $\delta\lambda > 400$ nm).

PACS numbers:

I. INTRODUCTION

Laser beam propagation is a critical component to high-energy density (HED) plasma physics. For example, in the indirect drive approach to inertial confinement fusion (ICF), laser beams are required to efficiently propagate through several millimeters of plasma before depositing high-power laser energy into a soft x-ray radiation field that drives the fusion capsule implosion by x-ray ablation pressure [1]. For achieving a symmetric capsule implosion and for reaching ignition conditions, it is required that the energetic laser beams efficiently propagate and create soft x rays close to where they were initially pointed. When the incident laser intensity is above the laser-plasma interaction thresholds, the available energy for x ray conversion is reduced through laser backscattering losses and the laser beams can be deflected by refraction, filamentation, or self focusing.

A transmitted beam diagnostic is used to study the under-dense plasmas that are inevitably produced at large laser facilities used to study HED plasmas. Measuring the laser beam transmission through these plasmas is important for understanding laser-plasma interactions and energetics. By measuring the transmitted power along with the standard backscatter diagnostics, an energy balance can be used to directly measure the laser beam absorption. Measuring the amount of light that is scattered outside of the original laser beam cone provides direct measure of filamentation; the intensity gradient in the incident laser beam profile produces a pondermotive force decreasing the density at the center of the beam. The resulting change in the index of refraction refracts the laser beam producing filaments.

The filamentation threshold for an ideal beam can be calculated by balancing the plasma pressure with the pondermotive force resulting from the profile of the laser beam [2]. A study using the laser-plasma interaction code

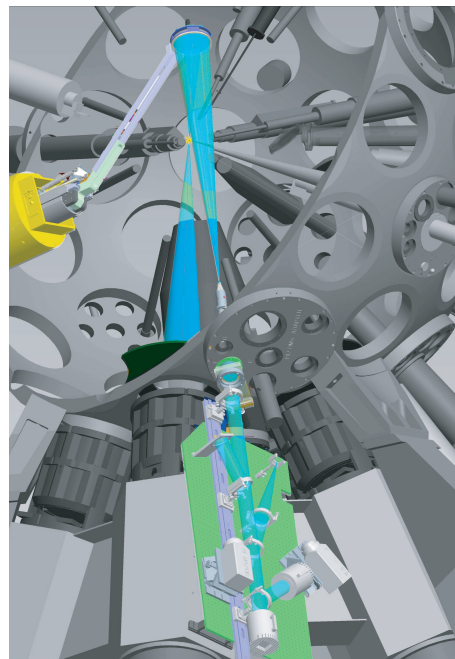


FIG. 1: Beam 30 propagates from through the target at TCC; light transmitted within twice the original f-cone is collected by a large focusing mirror suspended 60 cm from TCC. The light is directed out of the chamber onto a diagnostic platform.

Pf3d has extended this work to include a laser beam with a random phase plate (RPP) [?],

$$FFOM = \frac{I_p \lambda^2}{10^{13}} \left(\frac{n_e}{n_{cr}} \right) \left(\frac{3}{T_e} \right) \left(\frac{f\#}{8} \right)^2 \quad (1)$$

where I_p is the power averaged intensity at best focus, λ is the wavelength of the laser beam, n_e/n_{cr} is the fraction

of electron density to the critical density at 3ω , T_e is the electron temperature, and $f^\#$ is defined as the ratio of the focal length to the beam diameter. When the filamentation figure of merit (FFOM) is greater than one, the beam is predicted to experience significant filamentation and beam spray.

II. DIAGNOSTIC DETAILS

A 3ω transmitted beam diagnostic (3ω TBD) has been recently commissioned on the Omega Laser at the Laboratory for Laser Energetics, University of Rochester [3]. The 3ω TBD measures the light transmitted through the target chamber center (TCC) with in twice the original $f/6.7$ beam cone (Fig. 1).

Figure 1 shows the 3ω beam (B30) propagating 60 cm past TCC to a 25 cm diameter uncoated fused silica focusing mirror ($f = 44$ cm) that directs 4% of the transmitted light through a 4 inch diameter port (H17?) on the target chamber to a diagnostic platform. The focusing mirror is inserted through TIM5 (ten inch manipulator); the support and mirror block three laser beams: B41, B48, and B61. The majority of the transmitted light is absorbed by a beam dump directly behind the focusing mirror. A beam tube extends ~ 50 cm from the chamber wall to shield the diagnostics from a direct view of TCC.

On the diagnostic platform, a 4 inch diameter lens with a 65 cm focal length directs the light into two 4 inch diameter calorimeters (spects) that measure the transmitted energy in the spectral ranges above and below 400 nm. The lens produces a near field image of the transmitted light by imaging the plane of the the focusing mirror onto a spectralon plate [?].

1. Temporally Resolved Beam Spray and Incident Pulse Shape

Figure 2 shows the spectralon plate where 13 fiber ports have been installed. Each port has four 400 micron core multimode(?) UV grade optical fibers configured in a 1-mm diameter port that are used to spatially resolve the transmitted power and spectra.

Each of the 13 fiber locations are multiplexed into three fast photodiodes (Hamamatsu model number) by incrementally increasing the fiber optic cable length ($L=5$ ns). All three signals are recorded over a 100 ns time window with 3 channels from a 6 GHz Tektronics 6604B sampling oscilloscope (20 Gs/s); the system is capable of resolving a 100 ps Gaussian laser pulse.

The full transmitted beam and the incident laser pulse (B30) are multiplexed into the diodes. The system allows the transmitted power and incident pulse shape to be measured with no relative time jitter allowing accurate determination of the spatially and temporally resolved transmitted power fraction through the plasma.

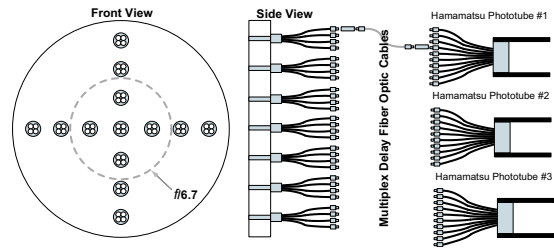


FIG. 2: The near field of the transmitted light is imaged onto a spectralon surface with 13 fiber optic ports used to sample the power and spectrum. The 3 cm diameter $f/6.7$ beam cone is shown as a dashed circle.

2. Spectral Measurements

The forward stimulated Raman scattering (FSRS) and forward simulated Brillion scattering (FSBS) are spectrally and temporally resolved at 5 independent locations selected from the 13 fiber ports. For each system, the light from each fiber travels through a delay fiber ($L=0$ ns, 2 ns, 4 ns, 6 ns, 8 ns) and then into five 4 meter (20 ns) jumpers where they are multiplexed [?] into a single 400 μm diameter core fiber that is coupled to a spectrometer.

FSBS employs a 1-meter Acton imaging spectrometer (AM-505). The input slit has been replaced by a 100 μm diameter core fiber optic cable. The spectral response of the system at 355 nm is $\text{FWHM}=x$ nm. A streak camera with a 30 ns time window is used to record the five temporally delayed spectra. The temporal resolution of the system is determined by the time shear introduced by the spectrometer which is estimated to be $\Delta t \sim \frac{Nm\lambda}{c} = 400$ ps where $N=3.6 \times 10^5$ is the number of groves on the grating that are illuminated, $m=1$ is the spectral order of the spectrometer, and c is the speed of light.

FSRS employs a 0.3-meter Acton imaging spectrometer (model). The input slit has been replaced by a 400 μm diameter core fiber optic cable. The spectral resolution of this system is $\text{FWHM}=x$ nm. A streak camera with a 30 ns time window is used to record the five temporally delayed spectra. The temporally resolved spectra are corrected for the dispersion in the fiber [4];

$$t(\lambda) = \frac{L_T}{c} \left[n(\lambda) - \lambda \frac{\partial n}{\partial \lambda} \right] \quad (2)$$

where L_T is the total fiber length, c is the speed of light in vacuum, and $n(\lambda)$ is the refractive index of the fiber core material. The quantity in brackets is defined at the group index N_g .

3. Time Integrated Beam Spray

Two gated optical 16-bit cameras (PI-MAX....) are used to measure the beam spray projected onto the spectralon plate. Twice the $f/6.7$ cone is imaged on to the

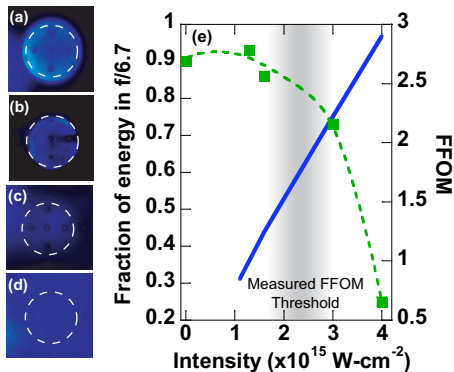


FIG. 3: (a) The interaction beam (B30) propagates through the system without a target to calibrate the system. (b) At an intensity of $1.6 \times 10^{15} \text{ W-cm}^{-2}$ the light is well contained within the original beam cone (dashed circle). (c) Light outside of the beam cone is observed for intensities above $3 \times 10^{15} \text{ W-cm}^{-2}$. (d) At the maximum intensity ($4 \times 10^{15} \text{ W-cm}^{-2}$), the laser beam has exploded and light is measured well past the beam cone. (e) The measured fraction of energy inside of the original $f/6.7$ beam cone (squares) decreases as the intensity increases above the filamentation threshold. The peak FFOM is calculated (line) using the parameters from hydrodynamic simulations.

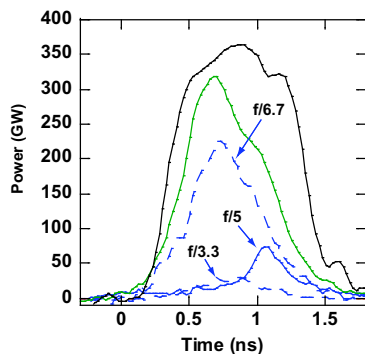


FIG. 4: The transmitted power is measured at three radii across the near field of the transmitted beam (Blue curves). Each curve is summed to give the total transmitted power (green curve). The incident laser power is measured with the same system (black curve).

cameras with two 105 mm $f/4.5$ achromatic (250 nm - 650 nm) lenses. The cameras are located 60 cm from the spectralon plate and the lenses demagnify the 3 cm diameter image of the beam cone projected onto the spectralon plate so that twice the beam cone fully illuminates the 1.2-cm diameter CCD (check specs in manual).

III. INITIAL TRANSMISSION RESULTS

An experiment to study the plasma in the laser entrance hole of an ignition hohlraum where the plasma temperature is expected to exceed 3.5 keV in a long-scale (2 mm) low-Z plasma ($n_e = 6 \times 10^{20} \text{ cm}^{-3}$) has recently been performed [5]. Figure 3 shows that the laser beam propagates through the plasma for intensities less than $2 \times 10^{15} \text{ W-cm}^{-2}$. Above this threshold, a large fraction of the energy is outside of the original beam cone. These measurements are compared in Fig. 3(e) with the peak FFOM determined by post-processing the parameters calculated by the hydrodynamic simulations performed by HYDRA [6] where the filamentation threshold is calculated to be at $I = 1.4 \times 10^{15} \text{ W-cm}^{-2}$; at this intensity there is no measured beam stray.

Figure 4 shows the temporal evolution of the beam spray for the high intensity laser shot shown in Figure 3(d). The temporal evolution at three radii are sampled ($f/6.7$, $f/5$, $f/3.3$). The total transmitted power is shown by adding each measurement and normalizing to the total measured transmitted energy. The transmission is compared to the incident pulse shape measured with the same system.

We have shown efficient laser beam propagation in 2-mm long high temperature plasmas that resemble the under dense fill plasma in an indirect drive fusion target. For intensities less than $2 \times 10^{15} \text{ W-cm}^{-2}$, 75% of the incident energy is transmitted with 90% of the energy in the original beam cone. When the plasma reaches its peak electron temperature of 3.5 keV, above 90% of the power is transmitted.

This work was supported by LDRD 06-ERD-056 and was performed under the auspices of the U.S. Department of Energy by the Lawrence Livermore National Laboratory under Contract No. W-7405-ENG-48.

-
- [1] J. D. Lindl, P. A. Amendt, R. L. Berger, S. G. Glendinning, S. H. Glenzer, S. W. Haan, R. L. Kauffman, O. L. Landen, and L. J. Suter, *Phys. Plasmas* **11**, 339 (2004).
 [2] A. J. Palmer, *Phys. Fluids* **14**, 2714 (1971).
 [3] J. M. Soures, R. L. McCrory, T. R. Boehly, R. S. Craxton, S. D. Jacobs, J. H. Kelly, T. J. Kessler, J. P. Knauer, R. L. Kremens, S. A. Kumpan, et al., *Laser Particle Beams* **11**, 317 (1993).
 [4] D. S. Montgomery and R. P. Johnson, *Rev. Sci. Instrum.*

- (2001).
 [5] D. H. Froula, P. F. Davis, B. B. Pollock, L. Divol, J. S. Ross, J. Edwards, R. P. J. Town, D. Price, S. H. Glenzer, A. A. Offenberger, et al., Submitted to PRL (2006).
 [6] M. M. Marinak, G. D. Kerbel, N. A. Gentile, O. S. Jones, D. H. Munro, S. Pollaine, T. R. Dittrich, and S. W. Haan, *Phys. Plasmas* **8**, 2275 (2001).